Received: 2 August 2022 | Revised: 15 September 2022 | Accepted: 27 September 2022

DOI: 10.1111/mpp.13275

Molecular Plant Pathology WILEY

SHORT COMMUNICATION

Heterologous expression of *Arabidopsis* pattern recognition receptor RLP23 increases broad-spectrum resistance in poplar to fungal pathogens

Lijuan Zhao | **Qiang Cheng**

Key Laboratory of Forest Genetics & Biotechnology of Ministry of Education, Co-Innovation Center for Sustainable Forestry in Southern China, Nanjing Forestry University, Nanjing, China

Correspondence
Qiang Cheng, Key Laboratory of Forest Genetics & Biotechnology of Ministry of Education, Co-Innovation Center for Sustainable Forestry in Southern China, Nanjing Forestry University, Nanjing 210037, China.
Email: chengqiang@njfu.edu.cn

Funding information
National Natural Science Foundation of China, Grant/Award Number: 31600512 and 31870658

Abstract

The pattern recognition receptor AtRLP23 from *Arabidopsis thaliana* recognizes the epitopes (nlp24s) of necrosis and ethylene-inducing peptide 1-like proteins (NLPs) and triggers pattern-triggered immunity (PTI). Here, we established methods for studying the early events of PTI in the hybrid poplar cultivar Shanxin (*Populus davidiana* × *Populus bolleana*) in response to the flagellin epitope. We confirmed that wild-type Shanxin cannot generate PTI responses on nlp24 treatment. Four NLP homologues were characterized from two common fungal pathogens of Shanxin, namely *Marssonina brunnea* f. sp. *monogermtubi* (MbMo) and *Elsinoë australis* (Ea), which cause black leaf spot and anthracnose disease, respectively, and the nlp24s of three of them could be responded to by *Nicotiana benthamiana* leaves expressing AtRLP23. We then created *AtRLP23* transgenic Shanxin lines and confirmed that the heterologous expression of AtRLP23 conferred on transgenic Shanxin the ability to respond to one nlp24 of each fungal pathogen. Consistently, infection assays with MbMo or Ea showed obviously lower levels of disease symptoms and significantly inhibited the growth of fungi on the transgenic poplar compared with that in wild-type poplar. Overall, our results indicated that the heterologous expression of AtRLP23 allowed transgenic Shanxin to generate a PTI response to nlp24s, resulting in increased broad-spectrum fungal disease resistance.

KEYWORDS
broad-spectrum resistance, nlp24, pattern recognition receptor, poplar cv. Shanxin, transformation

Plants use cell surface-localized pattern recognition receptors (PRRs) to recognize conserved pathogen-associated molecular patterns (PAMPs), leading to PAMP-triggered immunity (PTI) (Jones & Dangl, 2006). PTI activates a characteristic set of downstream responses, including extracellular alkalinization, an oxidative burst of reactive oxygen species (ROS), activation of mitogen-activated protein kinase (MAPK) cascades, deposition of callose, and expression of numerous defence-associated genes, that ultimately hinder pathogen proliferation, promoting basic immunity against adapted pathogens as well as nonadapted pathogens (Saijo et al., 2018). To date, more than 20 plant PRRs have been identified and most of them are restricted to certain plant groups/species (Tang et al., 2017). Multiple studies have shown that interspecies transfer of PRRs can enhance resistance to pathogens carrying the cognate PAMPs

in the recipient plants (Du et al., 2015; Hao et al., 2016; Lacombe et al., 2010; Tripathi et al., 2014).

Necrosis and ethylene-inducing peptide 1-like proteins (NLPs), widely distributed among bacteria, fungi, and oomycetes, especially those associated with plants, form a superfamily of microbial proteins. NLPs were first discovered as toxins to eudicot plants, but noncytotoxic NLP homologues also exist widely among plant-pathogenic microorganisms. The conserved 24-amino-acid region (nlp24) in type 1 NLPs, which include cytotoxic and noncytotoxic NLPs, is a PAMP that can induce immune responses in lettuce and some Brassicaceae family (Bohm et al., 2014; Oome et al., 2014). Recently, a leucine-rich repeat receptor-like protein (LRR-RLP), AtRLP23, from *Arabidopsis thaliana*, was identified as the PRR of nlp24 (Albert et al., 2015). Interspecies transfer of AtRLP23 to nlp24-nonresponsive potatoes conferred increased disease resistance to the fungal pathogen *Sclerotinia sclerotiorum* and the oomycete pathogen *Phytophthora infestans* (Albert et al., 2015).

Poplars (*Populus* spp.) are tree species that are widely cultivated worldwide because of their impressive growth performance and high productivity. Poplar plantations consisting of elite poplar clones provide important feedstock for producing fibreboard, paper pulp, and construction lumber, as well as forming shelterbelts against deserts and wind (Bradshaw et al., 2000; Tuskan et al., 2006). However, poplars are often affected by fungal foliar diseases, such as black leaf spot and anthracnose caused by *Marssonina brunnea* and *Elsinoë australis*, respectively, leading to premature leaf fall, reduced photosynthetic capacity, and decreased productivity (Han et al., 2000; Zhao et al., 2020).

So far, no PTI response events have been reported in poplar, and it is not known whether PTI can affect disease resistance in poplar. Here, we established experimental methods for the hybrid poplar cultivar Shanxin (*Populus davidiana*×*Populus bolleana*) to examine its PTI responses and confirmed that transformation with *AtRLP23* could increase the host resistance of Shanxin to its adapted fungal pathogens.

The PAMP flg22, a conserved 22-amino-acid peptide within the N-terminus of bacterial flagellins, can induce PTI responses in many plants. In contrast, the PAMP nlp24 has been found to induce PTI responses in only lettuce and some members of the Brassicaceae family. A rapid and transient oxidative burst is the hallmark of the PTI response, which can be detected within a few minutes by using a sensitive, luminol-based assay (Sang & Macho, 2017). First, we performed a luminol-based ROS assay with Shanxin leaf from 4- or 8-week-old transplanted tissue-cultured plantlets treated with 100 nM flg22. The magnitude of the ROS burst from 4-week-old plantlets was significantly higher than that from 8-week-old plantlets ($p < 0.01$) (Figure 1a). Figure 1b shows the ROS-burst curve generated within 60 min of flg22 treatment of leaf discs of 4-week-old

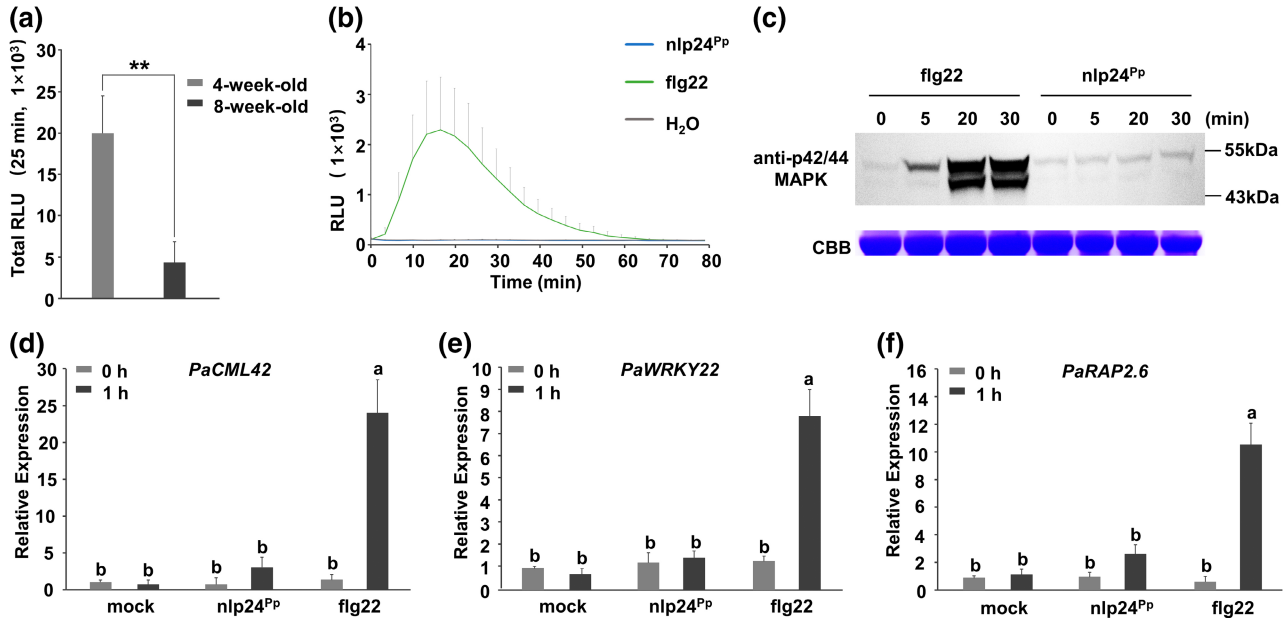

FIGURE 1 The immune responses of Shanxin poplar to PAMPs. (a) Reactive oxygen species (ROS) production of leaf discs from 4- and 8-week-old Shanxin transplanted tissue-cultured plantlets after flg22 (100 nM) treatment. Total relative light units (RLUs) for 25 min after treatment was calculated. Standard deviation (*SD*) calculation and significance analysis were derived from data of three independent experiments. $^{**}p < 0.01$ using Student's *t* test. (b) Kinetics of ROS production of leaf discs from 4-week-old Shanxin transplanted tissue-cultured plantlets in response to flg22 (100 nM) or $nlp24^{Pp}$ (1 μM). The error bars represent the mean ± *SDs* (leaf discs, $n = 8$). (c) MAPK activation in Shanxin leaf discs triggered by flg22 (1 μM) but not by $nlp24^{Pp}$ (1 μM), detected with a phospho-p44/42 MAPK antibody. The Coomassie Brilliant Blue (CBB)-stained gel shows representative loading amounts of each sample. (d–f) Expression pattern of *PaCML42*, *PaWRKY22*, and *PaRAP2.6* in Shanxin leaves induced by flg22 (1 μM) and $nlp24^{Pp}$ (1 μM). Bars indicate mean ± *SD* (independent experiments, $n = 3$). Different letters indicate statistically significant differences among mean values calculated using one-way analysis of variance followed by Tukey's test ($p < 0.05$).

plantlets, reaching its peak after 15 min; in contrast, on treatment with nlp24^{Pp} (1 μM) derived from PpNLP of *Phytophthora parasitica* and one of the prototypes of PAMP nlp24, no obvious ROS burst was observed in Shanxin.

Early elements of PTI in plants include activation of MAPK cascades after flg22 treatment, for example AtMPK6 and AtMPK3 of *A. thaliana* are phosphorylated within 10 min (Asai et al., 2002). We used a phospho-p44/42 MAPK antibody to detect MAPK activation in response to flg22 (1 μM) treatment on Shanxin leaf discs. The western blots revealed that one 48 kDa MAPK (close to the size of AtMPK6) was activated after 5 min of treatment (Figure 1c), whereas 20–30 min after treatment, another MAPK, 44 kDa (similar in size to AtMPK3), was activated (Figure 1c). In contrast, we were unable to observe MAPK activation after nlp24^{Pp} (1 μM) treatment of Shanxin leaf discs (Figure 1c).

Arabidopsis PTI response involves the reprogramming of a large number of genes, including some rapid-responding genes, such as *AtCML42* (At4g20780), *AtWRKY22* (AT4G01250), and *AtRAP2.6* (AT1G43160) (Göhre & Robatzek, 2008; Navarro et al., 2004), which we selected as marker genes to monitor PAMP recognition.

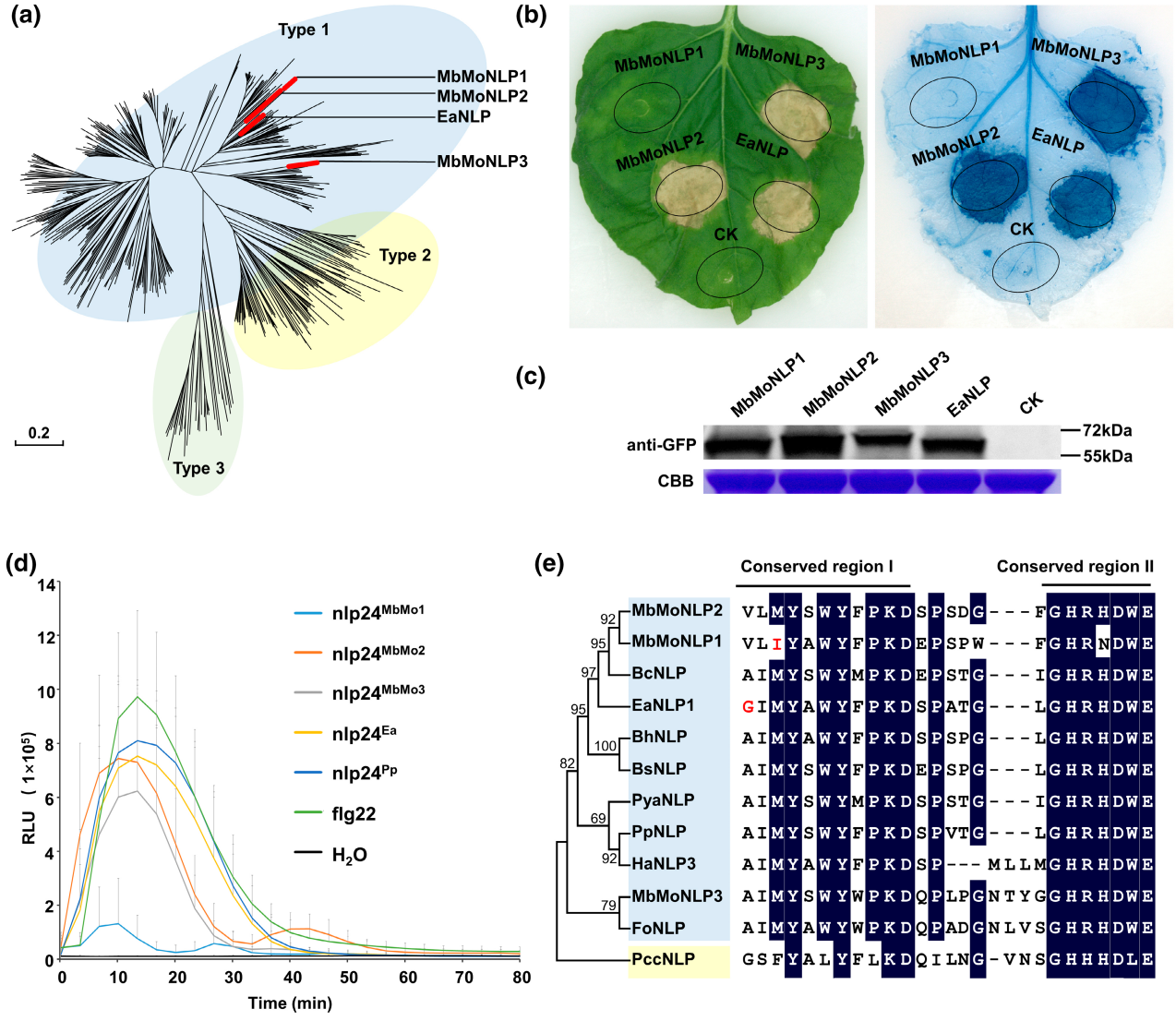

FIGURE 2 NLPs and nlp24 epitopes of adapted fungal pathogens of Shanxin poplar. (a) Phylogeny of 537 NLPs. The phylogenetic tree was constructed using the neighbour-joining (NJ) method. The branches of MbMoNLP1, MbMoNLP2, MbMoNLP3, and EaNLP are indicated in red. The blue, yellow, and green backgrounds represent type 1, type 2, and type 3 NLP clades, respectively. (b) Left panel: cell death induced by transiently expressed NLPs on a *Nicotiana benthamiana* leaf. Right panel: trypan blue staining to visualize cell death. The photograph was taken 4 days after *Agrobacterium* infiltration. CK, *Agrobacterium* with empty vector. (c) The expression of NLPs in *N. benthamiana* leaves was detected by western blotting, using an anti-GFP antibody. (d) Reactive oxygen species production triggered by PAMPs. The *N. benthamiana* leaf discs transiently expressing *AtRLP23* were inoculated with flg22 (100 nM) or various nlp24s (1 μM) (leaf discs, $n = 8$). (e) Phylogeny of eight NLP homologues and alignment of their nlp24s. The tree was constructed using the maximum-likelihood method and tested by 1000 bootstrap replicates. The blue background represents type 1 NLPs that have pathogen-associated molecular pattern (PAMP) activity in *Arabidopsis thaliana*. The yellow background represents type 2 NLP that has no PAMP activity in *A. thaliana*.

By BLASTp search against proteins of *Populus alba* (Liu et al., 2019) with these *Arabidopsis* PTI marker genes, we chose *PaCML42* (GenBank accession no. XM_035057842), *PaWRKY22* (XM_035031987), and *PaRAP2.6* (XM_035045539) for further verification. Using primers (Table S1) of these *P. alba* genes to amplify the cDNA of Shanxin, a single band of the correct target size could be observed (Figure S1). The reverse transcription-quantitative PCR (RT-qPCR) results showed that the expression levels of genes *PaCML42*, *PaWRKY22*, and *PaRAP2.6* were significantly up-regulated 1 h after 1 μM flg22 treatment; in contrast, no significant changes were found in the expression levels of these three genes after exposure to nlp24^{Pp} (1 μM) or water (mock treatment) (Figure 1d–f).

M. brunnea f. sp. *monogermtubi* (MbMo) and *E. australis* (Ea) are common fungal pathogens of Shanxin, and the genomes of these two fungi have been sequenced in our previous studies (Cheng et al., 2022; Zhao et al., 2020). A tBLASTn search with NLP of *P. parasitica* (GenBank accession no. AAK19753) against the genomes of these two fungi revealed that MbMo encodes three NLPs and Ea encodes one NLP, all of which contained signal peptides and conserved NPP1 domains (PF05630, E value <3.6e−52). We refer to them as MbMoNLP1 (OM964796), MbMoNLP2 (OM964796), MbMoNLP3 (OM964796), and EaNLP (PSK53154). Phylogenetic analysis combined with a collection of 533 NLP homologues (Oome & Van den Ackerveken, 2014) revealed that MbMoNLP1–MbMoNLP 3 and EaNLP belonged to the type 1 NLP clade (Figure 2a). The coding sequences of the four mature NLP proteins were amplified from the cDNA of poplar leaves infected by the two fungi for 4 days (Table S1). Sanger sequencing showed that the predicted introns were appropriately spliced, and the cloned sequences were all consistent with predicted gene models, indicating that the four *NLP* genes were not pseudogenes and were expressed in the early stage of infection. Then, we constructed binary vectors containing the CaMV 35S promoter to drive the mature NLP of the 5′ terminus fused to an *A. thaliana* PR1 signal peptide (*35S::AtPR1sp:NLPs*). Transient expression of these constructs in *Nicotiana benthamiana* leaves showed that MbMoNLP2, MbMoNLP3, and EaNLP induced clear cell death, although MbMoNLP1 did not (Figure 2b). Western blot analysis of transiently expressed *35S::AtPR1SP:NLPs:GFP* (where a green fluorescent protein tag was added at the C terminus) showed that all four NLP-GFP fusion proteins successfully accumulated

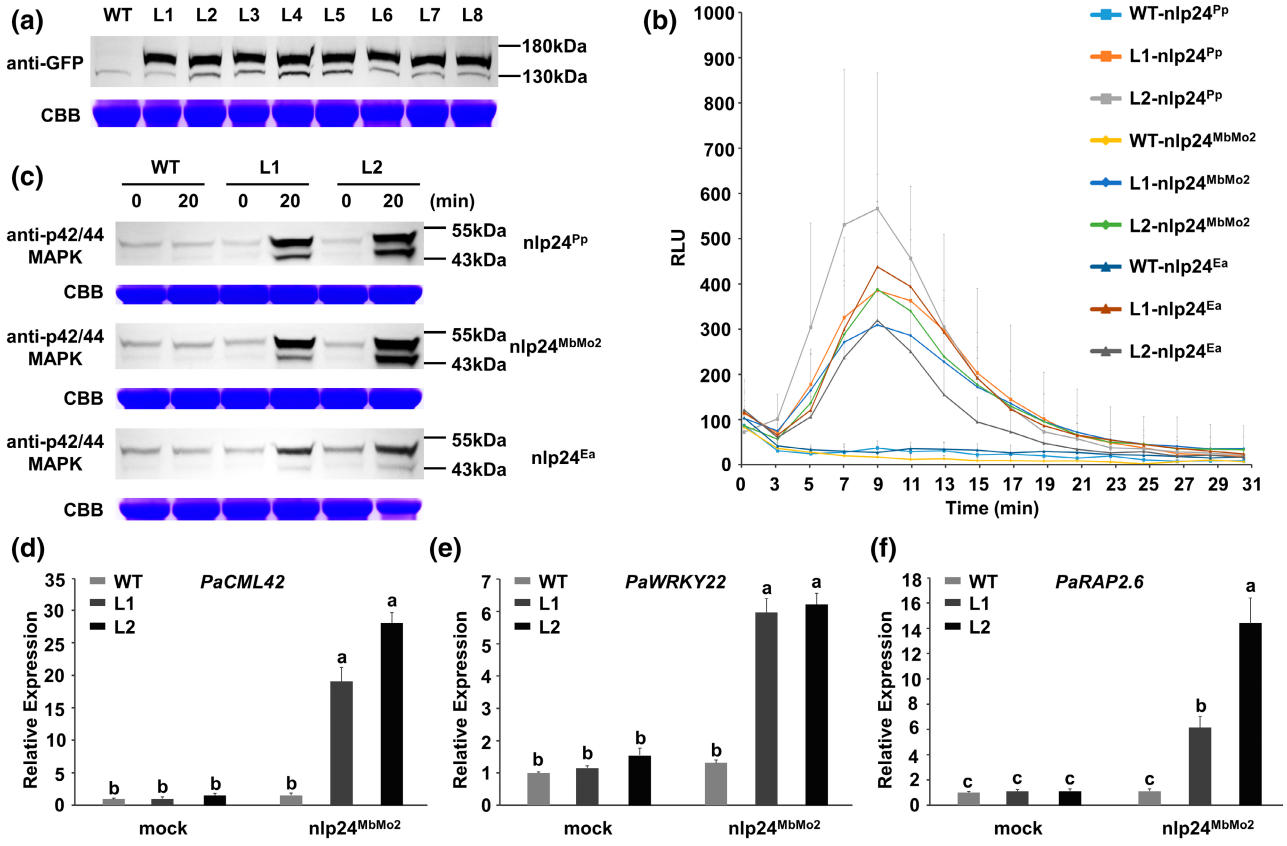

FIGURE 3 *AtRLP23* transgenic poplar Shanxin lines, which responded to nlp24s. (a) The expression of AtRLP23-GFP in transgenic lines of Shanxin leaves was detected by western blotting using an anti-GFP antibody. (b) Reactive oxygen species burst in transgenic lines L1 and L2 treated with 1 μM nlp24^{MbMo2}, nlp24^{Ea}, or nlp24^{Pp} but no response in the wild-type Shanxin (WT). (c) MAPK activation in transgenic lines L1 and L2 treated with 1 μM nlp24^{MbMo2}, nlp24^{Ea}, or nlp24^{Pp} but no activation in the wild-type Shanxin. (d–f) Expression of *PaCML42*, *PaWRKY22*, and *PaRAP2.6* in transgenic lines L1 and L2 induced by 1 μM nlp24^{MbMo2}; the wild-type Shanxin or mock (water) treatment of the transgenic lines were not induced. Expression levels were assessed at 1 h after treatment. Bars indicate the mean ± *SD* (from three independent experiments). Samples with different letters indicate statistically significant differences among mean values calculated using one-way analysis of variance followed by Tukey's test ($p < 0.05$).

(51–53 kDa) (Figure 2c). Meanwhile, we found that the ability of NLPs to induce cell death was significantly reduced by the introduction of the C-terminal GFP tag. Cell death induced by MbMoNLP2-GFP and EaNLP-GFP was nearly undetectable, and cell death induced by MbMoNLP3-GFP could be observed only in the centre of the *Agrobacterium*-infiltrated region (Figure S2) in the presence of the GFP tag.

The epitopes of MbMoNLP1, MbMoNLP2, MbMoNLP3, and EaNLP, that is, nlp24^{MbMo1}, nlp24^{MbMo2}, nlp24^{MbMo3}, and nlp24^{Ea}, were identified by alignment with nlp24^{Pp}. The peptides of nlp24$^{MbMo1-3}$ and nlp24^{Ea} were then synthesized and tested for ROS induction ability on Shanxin leaf discs. No ROS burst was found when using each of these synthetic peptides (Figure S3), which was consistent with the experimental result using nlp24^{Pp} (Figure 1b). *N. benthamiana* proved to be insensitive to nlp24^{Pp}, while the heterologous expression of AtRLP23-GFP could confer on *N. bethamiana* the ability to respond to nlp24^{Pp} (Albert et al., 2015). We found that *N. benthamiana* was also insensitive to nlp24^{MbMo1}, nlp24^{MbMo2}, nlp24^{MbMo3}, and nlp24^{Ea} (Figure S4), whereas, by transiently expressing *35S::AtRLP23:GFP* in leaves, *N. benthamiana* obtained the ability to respond to nlp24^{MbMo2}, nlp24^{MbMo3}, nlp24^{Ea}, and nlp24^{Pp}, but not nlp24^{MbMo1} (1 μM), producing an ROS burst at a level comparable to that induced by flg22 (100 nM) (Figure 2d). Oomea et al. have shown that the methionine-to-alanine mutation at the position 3 amino acid of nlp24^{HaNLP3} (derived from *Hyaloperonospora arabidopsidis* NLP3) significantly reduced its PAMP activity (Oome et al., 2014).

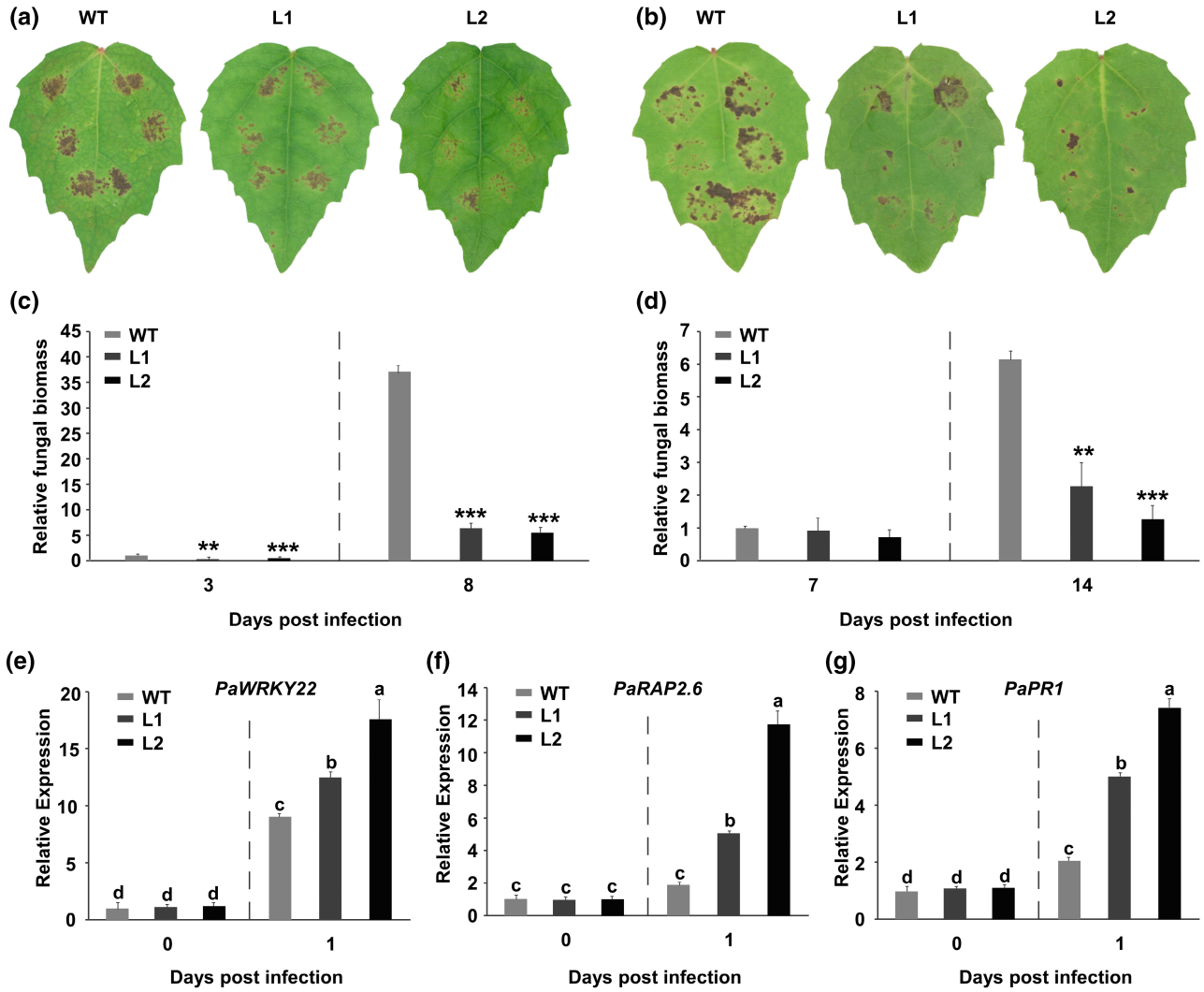

FIGURE 4 Transgenic poplar Shanxin lines L1 and L2 expressing *AtRLP23* show increased resistance to *Marssonina brunnea* f. sp. *monogermtubi* (MbMo) and *Elsinoë australis* (Ea). (a, b) Representative leaves inoculated with (a) MbMo and (b) Ea. Photographs were taken at (a) 8 and (b) 14 days postinoculation (dpi), respectively. (c, d) Fungal biomass of MbMo and Ea was determined by real-time quantitative PCR in transgenic lines L1 and L2, and the wild-type Shanxin (WT). Statistical differences compared with the wild type were determined using Student's *t* test (**$p < 0.01$, ***$p < 0.001$). Bars indicate the mean ± *SE* (from three independent experiments). (e–g) Expression pattern of *PaWRKY22* (e), *PaRAP2.6* (f), and *PaPR1* (g) in wild-type Shanxin and transgenic lines induced by MbMo infection at 0 and 1 dpi. Bars indicate the mean ± *SD* (from three independent experiments). Samples with different letters denote statistically significant differences among mean values calculated using one-way analysis of variance followed by Tukey's test ($p < 0.05$).

Alignment with the known nlp24 that has PAMP activity revealed that isoleucine at position 3 of nlp24^{MbMo1} was unique (isoleucine vs. methionine), which may be the reason why nlp24^{MbMo1} eluded AtRLP23 recognition (Figure 2e).

The above results imply that genetic transformation with *AtRLP23* might confer Shanxin with the ability to recognize nlp24s from its adapted pathogens. To test this hypothesis, we generated stable transgenic lines of Shanxin expressing *35S::AtRLP23:GFP* with the *Agrobacterium*-mediated transformation method. Western blotting with an anti-GFP antibody was used to detect the accumulation of AtRLP23. We observed a c.150 kDa protein band (subtracting GFP, c.120 kDa), consistent with the AtRLP23 molecular weight determined in *A. thaliana*, in eight transgenic Shanxin lines, but not in wild-type Shanxin (Figure 3a). Plantlets of transgenic lines L1 and L2 were tested for further analysis of effects on growth or morphology. Compared with wild-type Shanxin, incorporation of the transgene *AtRLP23* into lines L1 and L2 did not lead to any significant changes in growth or morphology of L1 and L2 (Figure S5). ROS assays revealed that L1 and L2 had developed the ability to respond to nlp24, resulting in an ROS burst reaching a peak approximately 10 min after treatment with nlp24^{MbMo2}, nlp24^{Ea}, or nlp24^{Pp} (Figure 3b). Western blot analyses showed that both the 48 kDa and the 44 kDa MAPKs were phosphorylated in the L1 and L2 transgenic lines within 20 min of treatment with nlp24^{MbMo2}, nlp24^{Ea}, or nlp24^{Pp} (Figure 3c). Furthermore, the expression levels of *PaCML42*, *PaWRKY22*, and *PaRAP2.6* in these two transgenic lines were significantly higher than those in the wild-type Shanxin poplar at 1 h after nlp24^{MbMo2} treatment and were also significantly higher than those in the transgenic lines and wild type at 1 h after mock (water) treatment (Figure 3d–f).

To confirm whether *AtRLP23* transformation could enhance Shanxin resistance to its adapted pathogens, we inoculated detached leaves of L1, L2, and wild-type Shanxin with MbMo (10^5 conidia/ml) and Ea (hyphal plugs). Disease-associated lesions on leaves of L1 and L2 caused by either fungus were clearly smaller than those on the wild-type poplar (Figure 4a,b). We evaluated fungal biomass using real-time qPCR. At both early (3 days postinoculation, dpi) and late infection stages (8 dpi) of MbMo, fungal biomass accumulation on transgenic lines L1 and L2 was significantly lower than that on the wild-type Shanxin (Figure 4c). In contrast, the significant decrease in Ea biomass on transgenic lines L1 and L2 was mainly observed at the late stage of infection (14 dpi but not 7 dpi) (Figure 4d).

As heterologous expression of AtRLP23 may affect the defence of Shanxin against MbMo in the early stage of infection, we used RT-qPCR to analyse the expression of PTI marker genes and *PR1*, a common marker gene in immune responses, in wild-type and transgenic lines at 0 and 1 dpi with MbMo. The results showed that the expression levels of *PaWRKY22*, *PaRAP2.6*, and *PaPR1* (XM_035062667) (Table S1) were up-regulated in both wild-type and transgenic lines at 1 dpi, but the expression levels of these genes in transgenic lines were significantly higher than those in the wild-type Shanxin (Figure 4e–g). This result implied that the increased resistance to MbMo in transgenic lines originates from enhanced early immune responses.

In summary, we established methods for detecting the early events of PTI in Shanxin poplar based on protocols used in *Arabidopsis* and confirmed that Shanxin could respond to flg22 but not to nlp24. We characterized the cytotoxicity and immunogenicity of four NLP proteins from two Shanxin-adapted fungal pathogens, MbMo and Ea. We further demonstrated that genetic transformation with *AtRLP23* could confer Shanxin with the ability to respond to nlp24 and significantly improve its resistance to MbMo *and* Ea. This study supports the conservation of the PTI signalling pathway between poplar and well-studied model plants, and the effectiveness of poplar PTI against fungal pathogens. Therefore, interspecies transfer of *AtRLP23* or other PRRs represents a promising strategy for breeding broad-spectrum and durable resistance in poplar trees. Shanxin, an economically important cultivar, is often affected by various fungal diseases. It is therefore necessary to further evaluate the resistance performance of *AtRLP23* transgenic lines in the greenhouse, as well as to optimize the promoters, to provide reliable information for the application of a field release permit.

ACKNOWLEDGEMENTS

This work was supported by the National Natural Science Foundation of China (grant no. 31870658) and the Natural Science Foundation of Jiangsu Higher Education Institutions of China (grant no. 21KJA220002).

DATA AVAILABILITY STATEMENT

The data that support the findings of this study are available from the corresponding author upon reasonable request.

ORCID

Qiang Cheng https://orcid.org/0000-0001-6759-2483

REFERENCES

Albert, I., Böhm, H., Albert, M., Feiler, C.E., Imkampe, J., Wallmeroth, N. et al. (2015) An RLP23–SOBIR1–BAK1 complex mediates NLP-triggered immunity. *Nature Plants*, 1, 15140.

Asai, T., Tena, G., Plotnikova, J., Willmann, M.R., Chiu, W.L., Gomez-Gomez, L. et al. (2002) MAP kinase signalling cascade in *Arabidopsis* innate immunity. *Nature*, 415, 977–983.

Bohm, H., Albert, I., Oome, S., Raaymakers, T.M., Van den Ackerveken, G. & Nurnberger, T. (2014) A conserved peptide pattern from a widespread microbial virulence factor triggers pattern-induced immunity in *Arabidopsis*. *PLoS Pathogens*, 10, e1004491.

Bradshaw, H.D., Ceulemans, R., Davis, J. & Stettler, R. (2000) Emerging model systems in plant biology: poplar (*Populus*) as a model forest tree. *Journal of Plant Growth Regulation*, 19, 306–313.

Cheng, Q., Yang, H., Chen, J. & Zhao, L. (2022) Population genomics reveals population structure and mating-type loci in *Marssonina brunnea*. *Journal of Fungi*, 8, 579.

Du, J., Verzaux, E., Chaparro-Garcia, A., Bijsterbosch, G., Keizer, L.C.P., Zhou, J. et al. (2015) Elicitin recognition confers enhanced resistance to *Phytophthora infestans* in potato. *Nature Plants*, 1, 15034.

Göhre, V. & Robatzek, S. (2008) Breaking the barriers: microbial effector molecules subvert plant immunity. *Annual Review of Phytopathology*, 46, 189–215.

Han, Z., Yin, T., Li, C., Huang, M. & Wu, R. (2000) Host effect on genetic variation of *Marssonina brunnea* pathogenic to poplars. *Theoretical and Applied Genetics*, 100, 614–620.

Hao, G., Pitino, M., Duan, Y. & Stover, E. (2016) Reduced susceptibility to *Xanthomonas citri* in transgenic citrus expressing the FLS2 receptor from *Nicotiana benthamiana*. *Molecular Plant-Microbe Interactions*, 29, 132–142.

Jones, J.D. & Dangl, J.L. (2006) The plant immune system. *Nature*, 444, 323–329.

Lacombe, S., Rougon-Cardoso, A., Sherwood, E., Peeters, N., Dahlbeck, D., van Esse, H.P. et al. (2010) Interfamily transfer of a plant pattern-recognition receptor confers broad-spectrum bacterial resistance. *Nature Biotechnology*, 28, 365–369.

Liu, Y.J., Wang, X.R. & Zeng, Q.Y. (2019) De novo assembly of white poplar genome and genetic diversity of white poplar population in Irtysh River basin in China. *Science China Life Sciences*, 62, 609–618.

Navarro, L., Zipfel, C., Rowland, O., Keller, I., Robatzek, S., Boller, T. et al. (2004) The transcriptional innate immune response to flg22. Interplay and overlap with Avr gene-dependent defense responses and bacterial pathogenesis. *Plant Physiology*, 135, 1113–1128.

Oome, S. & Van den Ackerveken, G. (2014) Comparative and functional analysis of the widely occurring family of Nep1-Like proteins. *Molecular Plant-Microbe Interactions*, 27, 1081–1094.

Oome, S., Raaymakers, T.M., Cabral, A., Samwel, S., Bohm, H., Albert, I. et al. (2014) Nep1-like proteins from three kingdoms of life act as a microbe-associated molecular pattern in *Arabidopsis*. *Proceedings of the National Academy of Sciences of the United States of America*, 111, 16955–16960.

Saijo, Y., Loo, E.P. & Yasuda, S. (2018) Pattern recognition receptors and signaling in plant–microbe interactions. *The Plant Journal*, 93, 592–613.

Sang, Y. & Macho, A.P. (2017) Analysis of PAMP-triggered ROS burst in plant immunity. *Methods in Molecular Biology*, 1578, 143–153.

Tang, D.Z., Wang, G.X. & Zhou, J.M. (2017) Receptor kinases in plant–pathogen interactions: more than pattern recognition. *The Plant Cell*, 29, 618–637.

Tripathi, J.N., Lorenzen, J., Bahar, O., Ronald, P. & Tripathi, L. (2014) Transgenic expression of the rice *Xa21* pattern-recognition receptor in banana (*Musa* sp.) confers resistance to *Xanthomonas campestris* pv. *musacearum*. *Plant Biotechnology Journal*, 12, 663–673.

Tuskan, G.A., DiFazio, S., Jansson, S., Bohlmann, J., Grigoriev, I., Hellsten, U. et al. (2006) The genome of black cottonwood, *Populus trichocarpa* (Torr. & Gray). *Science*, 313, 1596–1604.

Zhao, L.J., Xiao, H.J., Ma, X.J. & Cheng, Q. (2020) *Elsinoë australis* causing spot anthracnose on poplar in China. *Plant Disease*, 104, 2202–2209.

SUPPORTING INFORMATION

Additional supporting information can be found online in the Supporting Information section at the end of this article.

How to cite this article: Zhao, L. & Cheng, Q. (2023) Heterologous expression of *Arabidopsis* pattern recognition receptor RLP23 increases broad-spectrum resistance in poplar to fungal pathogens. *Molecular Plant Pathology*, 24, 80–86. Available from: https://doi.org/10.1111/mpp.13275